Modeling Earth Systems and Environment (2026) 12:132
https://doi.org/10.1007/s40808-026-02779-8

ORIGINAL ARTICLE

A physically-based conceptual model calibrated on experimental data for estimating the flood instability hazard for pedestrians in urban area

Raffaele Albano[1] · Ruggero Ermini[2] · Tommaso Moramarco[3] · Aurelia Sole[4,5]

Received: 6 January 2026 / Accepted: 23 March 2026 / Published online: 1 April 2026

Abstract

Urban flood events pose significant risks to pedestrian safety. Analyzing pedestrian stability, during those events, enables the correlation of hazard levels with flood dynamics, which helps to identify critical areas and suggest evacuation routes. The present study introduces a novel approach for determining instability-thresholds for pedestrians during urban flooding. The methodology is based both on instability unit strength and specific energy—two fundamental hydraulic parameters that influence the balance of a body affected by fluid flow actions. The approach employs a physically-based formula that incorporates three calibration factors to balance the static and dynamic components of pedestrian stability, resulting in a conceptual instability threshold curve optimized by fitting a dataset of 417 experimental literature cases. By combining flow velocity and water depth, we identified a graph that identifies three hazard levels. These levels were obtained by minimizing the model's prediction errors and show areas where pedestrians are at the highest risk of being swept away. The proposed identification of critical thresholds was applied to the urban areas of Matera in the Basilicata Region of South Italy. This case study aimed to demonstrate the method's effectiveness and its ability to provide valuable insights for flood management. By pinpointing flood-prone roads, warning areas, and safe evacuation routes, this approach supports emergency response efforts, enhances flood preparedness, and ultimately improves public safety during flooding events.

Keywords Pedestrian stability · Flood instability · Urban flood risk · Risk thresholds

Introduction

Based on the Atlas of Human Planet (European Commission - Joint Research Centre et al. 2024), exposure to major natural hazards has significantly increased globally, partly due to urbanization's growth and spread. Therefore, it is crucial to identify the most effective measures to mitigate the impact of extreme events while taking ongoing global climate change into account (IPCC 2022). At the international level, the Framework for Disaster Risk Reduction 2015–2030, promoted by the United Nations Office for Disaster Reduction, with its seven global objectives, has highlighted the need to enhance our understanding of natural risk factors to improve societal resilience and reduce the consequences of natural disasters (UNISDR, 2015). The Flood Risk Management Plan, established by the European Directive 2007/60/EC, mandates the implementation of structural and non-structural interventions to manage flood risks in areas deemed to have significant potential risks, aiming to

✉ Raffaele Albano
raffaele.albano@unibas.it

Ruggero Ermini
ruggero.ermini@unibas.it

Tommaso Moramarco
tommaso.moramarco@cnr.it

Aurelia Sole
aurelia.sole@unibas.it

[1] Department of Health Science, University of Basilicata, Potenza, Italy

[2] Department for Humanistic, Scientific, and Social Innovation, University of Basilicata, Matera, Italia

[3] Research Institute for Geo-Hydrological Protection - IRPI, CNR, Perugia, Italy

[4] Department of Engineering, University of Basilicata, Potenza, Italia

[5] Research Institute of Hydrological Protection - IRPI, CNR, Cosenza, Italia

mitigate potential negative consequences for human health, affected territories, assets, the environment, cultural heritage, and economic and social activities.

However, despite many advancements in regulations and legislation, the impacts (and frequency) of flood events in Europe and worldwide have increased (Winsemius et al. 2016). This phenomenon is complex, involving interacting actions to climate change, land cover and land use transformations, and the ability of population to perceive risks and adopt self-protection actions (Jonkman and Penning-Rowsell 2008). Indeed, individual behaviors—such as walking in flooded areas or crossing river bridges—can be decisive during flood events (Albano et al. 2015).

Often People tend to underestimate the hazard in flood-prone areas, typically, due to a misunderstanding of the impact that a fast-moving flood wave can have on the human body, especially in shallow water (Lechowska 2018). Given that flood risks cannot be completely eliminated and that human behaviors are often linked to low-risk literacy (perhaps due to the rare occurrence of extreme events and the weak memories they leave) these phenomena can be very threatening. Instead of moving away from floods or staying in safe areas, individuals often face unnecessary risks, attempting to save objects, cars, or drive through flooded areas. These behaviors, along with the extreme characteristics of specific areas (such as small and steep river basins or watersheds prone to flash floods), emphasize the necessity for preventive measures and actions, particularly in urban settings.

In this context, it is crucial to complement traditional forecasting, alert, and emergency management systems with new methods and systems for risk communication and enhancing community resilience. For example, operational systems should be capable of identifying, in real-time, pedestrian and vehicular routes at risk, along with providing evacuation route indications due to rising floodwaters in urban areas (Albano et al. 2014; Sole et al. 2013). People's stability and safety can be compromised during extreme rainfall events, affecting their ability to stand, move, or escape from highly critical areas. Analyzing individual stability can be closely correlated with the hazard level of a flood event and its spatial-temporal dynamics, allowing for the identification of potentially critical areas and the evaluation of necessary self-protection measures and actions for various contexts and situations. This approach enables the development of predictive tools based on methodologies that assess the hazards and vulnerabilities of individuals exposed to hydrodynamic conditions that could lead to instability, while recognizing safe areas in contrast to critical conditions.

This study introduces a novel idea to identify specific criticality thresholds (instability-stability) for individuals exposed by flooding phenomena in urban areas. The research is based on a comprehensive analysis of both experimental and field data gathered from various researchers who have investigated this topic. A critical comparison of different methodologies is conducted to characterize the factors most influencing pedestrian stability and instability. Furthermore, to support emergency management efforts the study proposes a technical and practical framework to identify various flood hazard levels for pedestrians. This framework is applied to a case study in the historical center of Matera (Southern Italy), in order to demonstrate its effectiveness in identifying urban roads most susceptible to flooding during an event, highlighting areas that need timely warnings, and delineating safe evacuation routes. By integrating these insights, the study enhances urban flood response strategies and ultimately improve public safety.

Materials and methods

Experimental data on people affected by flood water

The stability and instability of floodwaters, or the incipient velocity experienced by adults (both men and women) and children, have been examined in various studies (see details in Table 1). These evaluations were conducted under controlled conditions through simulations in laboratory channels. Additionally, some hydraulic characteristic values associated with individuals swept away by floods were derived from photos and videos of historical flood events available on the web and social media.

The analyzed hydraulic parameters cover a range of diverse scenarios and conditions, influencing both individual perception and the impact of the flow on humans with varying physical characteristics and experimental scale. Specifically:

- Flood wave velocity, v, and water depth, h, exhibit significant dispersion values involving in the most cases clear water and absence of debris;
- Laboratory experiments conducted under a variety of conditions include safe environments (harnesses and optimal daylight conditions for lighting); moreover, some experiments utilize trained adult stunt performers in peak physical condition, while others are focused on children of various ages and sizes to capture a broader range of responses; additionally, scale models of pedestrians were also employed, dressed in different types of clothing (particularly various styles of shoes) to evaluate the influence of attire on stability;

Table 1 Summary of the review of experiments extracted from literature studies

Authors	Year	Setting	Setting Surface	Slope of the Setting	Subjects involved	Doing of the Subjects	Type of falling mechanism	Number of subjects	Range of variation of h [m]	Range of variation of v [m/s]
Foster, D.N., Cox R.	1973	Channel	Painted wood	Horizontal	Children (9–13 years)	Standing, walking, turning or sitting	The subject feels insecure or loses balance	6	0.11–0.24	2.2–3.08
Abt S.R. et al.	1989	Channel	Concrete, gravel and steel	-	Adults with safety equipment	Standing, walking or turning	Subject loses balance	20	0.43–1.21	0.74–2.77
Takahashi et al.	1992	Funnel Tank	Metal	Horizontal	Adults	Standing	Subject loses balance	3	0.46–0.84	0.88–1.83
Karvonen et al.	2000	Mobile channel	Steel grate	Horizontal	Rescuers with safety equipment	Standing, walking or turning	Subject loses balance	7	0.41–1.13	0.54–2.36
Yee, M.	2003	Channel	Wood	Horizontal	Children	Standing and walking	The subject feels insecure or loses balance	4	0.2–0.54	0.89–2.12
Jonkman and Penning-Rowsell,	2008	Channel	-	1%	Stuntman without safety equipment	Standing and walking	-	1	0.26–0.36	2.18–2.81
Russo	2013	Platform that simulates a street	Concrete	0-2-4-6-8-10%	Adults and Childrens	Standing, walking or turning	The subject feels insecure or loses balance	23	0.07–0.14	1.81–2.88
Xia et al.	2014	Channel	Concrete	Horizontal	Adult Human body model	Standing	Sliding or toppling	1	0.13–0.64	0.75–3.96
Chanson and Brown	2014	Urban street	Asphalt	Horizontal	Untrained adult with safety equipment	Standing and walking	The subject feels insecure or loses balance	3	0.41–0.96	0.46–0.47
Martinez-Gomariz et.al	2016	Platform that simulates a street	Concrete	0-2-4-6-8-10%	Adults and Childrens with safety equipment	Standing	The subject loses balance completely or partially	26	0.07–0.15	1.93–3.35
Milanesi et al.	2016		Real Environment	-	Adults and Childrens	Standing	Sliding, toppling or drowning	125	0.04–1.09	0.72–4.2
Zhu	2023	Channel	-	Horizontal	Child and Adult Human body model	Standing	Toppling	5	0.2–1.18	0.31–1.92

- The position and orientation of the flood water consider different flow angles and horizontal or inclined channel's surface.

It is worth noting that instability is heavily influenced by multiple "non-hydraulic" parameters. These include human and environmental factors, such as the psychophysical characteristics of the subjects (e.g., weight, height, body shape), dimensions, mass, balance, strength, foot size, mood, and physical responses. Additionally, climatic conditions (such as darkness, temperature, and rain), environmental risks (like water turbidity and debris), and experimental conditions (including channel slope and road incline) play a critical role.

Milanesi et al. (2015 and 2016) analyzed various videos available online showing people at risk during historical flood events, obtaining 125 cases of children (2.4%), teenagers (2.4%), and adults (95.2%) stability and instability. Finally, they estimated water depth and velocity values associated with the pedestrians (in-)stability conditions.

Foster and Cox (1973) tested the stability of barefoot children aged 9–13 years in an experimental channel, using a single type of shoe sole and having the children wear only in swimsuits, thus minimizing the interaction between clothing and current flow.

Abt et al. (1989) in their experiments used well-trained adults with safety equipment, conducting multiple repeated experiments resulting in an increasing of preparation and training as they repeat the tests. These situations are more representative of instability due to toppling considering that water depth values range between 0.4 and 1.2 m.

The study by Takahashi et al. (1992) for different h-v combinations tested instability of adults positioned orthogonally to the water flowing along a horizontal surface in case of different surface roughness and shoe types which friction coefficient are close to 0.4.

In the study by Karvonen et al. (2000), the dataset takes into account a wide range of h and v in order to represent both sliding and toppling instability failure mechanisms. The adults participating in the experimentation had the opportunity to familiarize themselves with the structures used and moved on a horizontal platform.

The experimental points obtained from Yee (2003) work concern children walking on a horizontal surface, both in static and dynamic conditions: the potential instability was associated with the loss of balance and insecurity.

Tests conducted by Jonkman and Penning-Rowsell (2008) in a full-scale channel with a constant slope of 1% involved a trained adult stuntman who was asked to walk in the flow without safety harnesses. Since the h was around 0.3 m and v over 2.4 m/s, the dataset could be considered a representative benchmark for sliding and drowning instability conditions.

The dataset of Xia et al. (2014) were performed in a horizontal channel using a human body physical model of 30 cm size and 0.334 kg weight, that in scale could be representative of a people of 1.70 m and 60 kg. Tests were conducted with the model maintained in a standing position both (i) facing the incoming flow direction and (ii) with the back of the body facing the flow direction.

Russo et al. (2013) tested the stability of adults in typical urban flood conditions where v are high and predominant over water levels, thus representing sliding and drawing instability conditions, with slopes up to 10%. Test results identify complete or partial loss of people balance for v exceeding 1.75 m/s even if the h is less than 0.2 m.

Chanson and Brown (2014) used three un-trained adult male researchers with safety equipment along a flooded road in horizontal surface conditions. The tests took place in an urban environment following a flood that affected the city of Brisbane, Australia, with h between 0.1 and 1 m and v between 0.0065 and 0.45 m/s.

Zhu et al. (2023) conducted experimentation with small-scale physical models of the human body to represent pedestrians in a nearly natural state, testing instability thresholds in a controlled channel. Five dummies were built and used: (a) a male model, (b) a female model wearing high heels, (c) a standing child model, (d) a male child model with legs diverging perpendicularly to the incoming flow and arms bent forward; (e) a male child model with legs diverging along the incoming flow, the right arm swinging forward, the left arm backward, and the body leaning forward. In addition to the five models previously mentioned, tests were also conducted based on body orientation concerning the flow direction, using the male model as the test object for 0°, 45°, 90°, and 180°.

The variability in experimental conditions across studies highlights the complexity of researching this topic within diverse human and environmental conditions.

The type of surface plays a crucial role in stability, particularly in terms of traction and friction, which affect a subject's ability to maintain balance. For example, Foster and Cox (1973) utilized painted wood, while Abt et al. (1989) studied concrete and gravel. Unconventional settings, such as funnel tanks and simulated street platforms examined in research by Takahashi et al. (1992) and Russo (2013), further broaden the importance of the roughness characteristics.

Additionally, participant demographics varied significantly across studies, with some involving children (Foster and Cox 1973; Yee 2003) and others focusing on adults equipped with safety gear (Martinez-Gomariz et al. 2016). This diversity can influence balance dynamics and affect how subjects respond to similar conditions.

Furthermore, the studies employed a range of slope variations, from horizontal (Chanson and Brown 2014) to inclined surfaces with variable slopes (Martinez-Gomariz et al. 2016). The local slope can preferentially influence types of instability, promote toppling and slipping mechanisms while limiting instances of drowning.

The activities subjects engaged in—standing, walking, or turning—also contributed significantly to in-stability mechanims. For instance, walking may introduce more dynamic instability compared to standing still, thus altering the reporting of incidents related to balance, such as losing balance (Abt et al. 1989) and sliding (Xia et al. 2014).

Finally, variations in sample sizes across different experiments, ranging from 1 to 125 participants, underscore the necessity of integrating datasets to enhance reliability across different conditions. Overall, the utilization of all the type of experiments may provide a more comprehensive understanding of pedestrian stability in various conditions making the identification of instability threshold more generalizable to different environmental and human conditions.

Table 1 lists all the literature studies from which the pairs of flow depth-velocity (h-v) values have been extracted. These values are compiled and harmonized into a single dataset, categorized into two classes, i.e. pedestrians' instability and stability, as illustrated in Fig. 1.

Despite the collection of 417 tests and observations, obtaining a data-driven synthetic or empirical identification of risk regimes remains challenging. Figure 1 illustrates the analyzed h-v combinations: 318 correspond to conditions of instability or incipient movement, while 99 refer to pedestrian flood stability. The data encompass tests conducted on 351 adults, 3 teenagers, and 63 children, with water depths ranging from a few centimeters to over 1 m. Specifically, h start at 0.04 m, as noted in the study by Milanesi et al. (2016), and reach up to 1.2 m in the research by Abt et al. (1989). The v varies between 0.31 and 4.2 m/s. Russo (2013) and Martinez-Gomariz et al. (2016) considered v exceeding 1.75 m/s, with h ranging from 15 to 20 cm, that is a typical condition of urbanized environments where floodwaters primarily flow along road channels, often characterized by significant slopes, particularly in cases of undersized or malfunctioning drainage systems.

Tolerable thrust associated with specific energy S/B*: a physically based conceptual model for estimating the instability of people affected by flood

During urban flood events, individuals are at significant risk of being swept away or drowning due to the combined effects of water depth, h, flow velocity, v, and the spatial and temporal dynamics of these parameters. The primary mechanisms of instability include toppling and sliding; however, the phenomenon of dragging also plays a crucial role, particularly when the water's energy is sufficient to lift a pedestrian. Often, the hazards faced by pedestrians arise from a combination of these factors (Milanesi et al. 2016). Toppling instability occurs when the force exerted

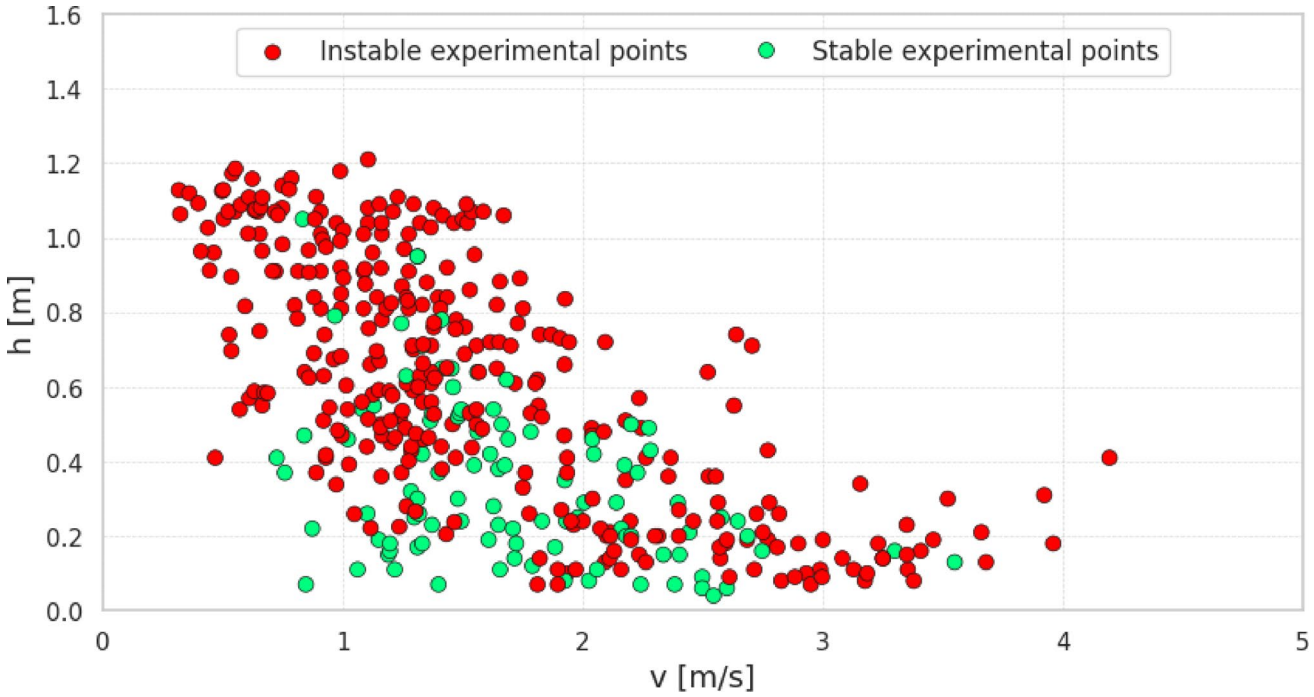

Fig. 1 Experimental points extracted form literature and divided into pedestrian stability and instability

by flood waters on a pedestrian, manifested as horizontal and/or vertical hydrodynamic forces, exceeds the effective body weight resistance of the individual. This resistance is influenced by factors such as the pedestrian's position relative to the main direction of the water flow and the slope of the road (Arrighi et al. 2017). Rotational stability and dragging also involve energy transfer from the water flow to the pedestrian, specifically the work done by the flow to shift the individual.

Sliding instability, which is characteristic of conditions with high flow velocities and low water depths, arises when the force of the flood flow acting on a person surpasses the friction force between the pedestrian's feet and the ground surface. The resistance to sliding for an individual is determined by the balance between the hydrodynamic force aligned with the water flow, the friction of the pavement, and the weight forces acting along the flow direction, particularly when the ground is inclined.

In this context, several authors (e.g., Russo et al. 2013; Xia et al. 2014; Zhu et al. 2023) have proposed synthetic methods that rely on expert judgments or empirical models, directly linking hydraulic variables with available experimental data. However, these methods often face limitations due to a partial or non-homogeneous sample of measurements, which can undermine the reliability of the results in different contexts and under new conditions, particularly when calibration data is scarce.

In contrast, physically based models enable researchers to enhance their understanding and retain control over the entire damage assessment process. Conceptual models, in particular, rely on a physical-mechanical analysis of the phenomena to establish more generalized safety criteria applicable during floods. The goal is to integrate these models into numerical and hydrodynamic frameworks that can quantify hydraulic hazards and risks, thereby effectively identifying critical areas within complex urban environments. Most models presented in the literature (e.g. Milanesi et al. 2016; Arrighi et al. 2017; Lazzarin et al. 2022) utilize simple equations to balance hydrodynamic forces, yet they exhibit varying degrees of complexity based on the number of parameters required to accurately describe the human and environmental conditions during the interaction between floodwaters and individuals.

A rigorous procedure that provides a fairly complete representation of the body's behaviour in water is the one proposed by Milanesi et al. (2015). In this study, the human body is modelled using cylindrical shapes and represented in an upright position on an inclined plane, where it impacts the flow directly. Given the inclined support surface over which the water flows, the body's weight, acting at the center of mass, is geometrically divided into a normal component and a parallel component relative to the surface. The buoyancy force, by contrast, acts vertically. The hydrodynamic force resulting from the fluid current operates in the direction of the flow and can be decomposed into components that are both parallel and orthogonal to the surface, while the friction force between the shoe soles and the ground is represented by the product of the friction coefficient and the effective weight, calculated as the algebraic sum of the forces normal to the sliding surface. This framework allows for the consideration of three different mechanisms of instability: sliding, toppling, and drowning. These mechanisms facilitate the evaluation of the minimum depths associated with each scenario: the minimum among the sliding (*hs*), toppling (*ht*), and drowning (*hd*) depths. In particular, sliding instability occurs when the sum of the drag force and the parallel component of the weight exceeds the friction force. Toppling instability arises when the moment generated by the normal component of the weight is overcome by destabilizing moments due to lift, drag, buoyancy, and the parallel component of the weight. Drowning is defined by a maximum allowable water depth, typically corresponding to the height of an individual's neck.

In the study conducted by Lazzarin et al. (2022), the authors propose a model based on a single dimensionless impact parameter W obtained from the combination of flow energy per unit weight, H, and momentum per unit width and weight, M:

$$H = h + \frac{v^2}{2g} = h\left(1 + \frac{1}{2}F^2\right) \tag{1}$$

$$M = \frac{h^2}{2} + \frac{v^2 h}{g} = \frac{h^2}{2}\left(1 + 2F^2\right) \tag{2}$$

where g is the gravity acceleration and $F = v(gh)^{-1/2}$ is the Froude number. Due to the similarity between the two expressions in Eq. 1 and Eq. 2, Lazzarin et al. (2022) introduced the general impact parameter W:

$$W = \left(\frac{h}{h_w}\right)^{\alpha}\left(1 + \beta F^2\right) \tag{3}$$

where h_W is a reference depth that scales the actual water depth h, and α and β are two calibration factors that measure, respectively, the relative importance of the static component compared to the dynamic component of W.

The key idea is that, with appropriate calibration factors, the iso-W lines in the h-v plane can identify different equivalent flow conditions in terms of potential criticality for specific categories of objects and processes. The method proposed by Lazzarin et al. (2022) evaluates damage functions solely in relation to flow-related factors, such as energy and momentum. As a result, it partially diverges

from the concept of pedestrian stability and instability in urban environments, especially given the multitude of variables involved—such as the height of the person or object being transported—which significantly alters the stability curve patterns without providing direct support for emergency management by generating alert thresholds.

Building on a critical analysis of the methodologies described above, this study introduces a different approach that defines the hydrodynamic threshold associated with a specific value of specific energy. This approach considers the mechanical action of a current along with the thrust and energy involved. Indeed, the thrust per unit width and specific energy are fundamental hydraulic parameters that regulate the balance of a body subjected to a fluid current (Moramarco 2011).

The thrust counteracts the resistance of the pedestrian or object, thus:

$$S = \rho Q v + \gamma A h_b \tag{4}$$

with S total thrust, Q flow rate, v flow speed, $\gamma = \rho g$ specific weight of the liquid, ρ density, g gravity acceleration, $A = h_b B$ area of the liquid section with h_b sinking of the body's center of gravity below the free surface, and B flow width.

From (4), the unit thrust can be inferred as:

$$\frac{S}{B} = \gamma h^2 (1 + F^2) \tag{5}$$

F is the Froude number.

The unit thrust *S/B* can be associated with the specific energy E of a flow characterized by a depth h and a speed v:

$$E = h + \frac{v^2}{2g} \tag{6}$$

Rewriting Eq. (4), the expression of speed as a function of parameters h and *S/B* is obtained:

$$v = \sqrt{\frac{g}{h}\left(\frac{S}{B\gamma} - \frac{1}{2}h^2\right)} \tag{7}$$

In order to identify the energy value corresponding to a given unit thrust, assuming $v = 0$, it is sufficient to estimate the value of h from (5) and substitute it into (6), thus obtaining the corresponding energy value.

Similarly, from Eq. (6), fixing e.g. E associated with a specific value of *S/B*, we get:

$$v = \sqrt{2g(E - h)} \tag{8}$$

Figure 2a shows the values of h and v, evaluated for predefined values of *S/B* and E, using Eqs. (5) and (6), respectively.

Therefore, the reference threshold for identifying the marginality limit is that associated with the lowest value of $h = \mathrm{h}(v)$ in the h-v plane, estimated through the combination of the curves such as shown in Fig. 2a.

Equation (5) can be rearranged incorporating the generalized parameters α, β, and C:

$$\frac{S}{B^*} = \frac{h^\alpha}{C}\gamma\left(1 + \beta F^2\right) \tag{9}$$

where *S/B** represents the tolerable thrust associated with specific energy, which describes hydrodynamic forces through a unified parameter. Moreover, the calibration factors α and β quantify the relative importance of the static component versus the dynamic component of *S/B*. They also express physically relevant concepts: flow energy, E (with $\alpha = 1$ and $\beta = 0.5$), and unit thrust *S/B* (with values of α and β equal to 2). This approach allows α and β to improve the shape of *S/B** to better fit the experimental dataset. Finally, the parameter C represents a reference value dependent on the water depth, wich incorporates the influence of an individual's height on the assessment of the instability threshold. In particular, Fig. 2b and c illustrate that the instability curves converge towards the energy and thrust models, respectively, by varying one at a time the values of α or β while keeping the other calibration parameters constant.

The Fig. 2d shows how the instability curve shape changes as function of C parameter keeping α and β constant.

Hazard for pedestrian in flood water

The primary goal is to improve the accuracy of the *S/B** curve by applying appropriate calibration factors, thereby achieving a better fit to the experimental data collected. To this end, the dataset was randomly divided into two subsets while maintaining the proportional distribution of stable and unstable points: 80% of the data was used for calibration, during which the S/B* curves and their associated calibration parameters were estimated to optimally fit the data. The remaining 20% served as a validation set, allowing for an independent assessment of the calibrated curves' performance. This approach facilitates benchmarking different curves and identifying the most reliable one for predicting experimental observations. Randomly generating multiple subsets within the calibration and validation classes, while maintaining the ratio of stable to unstable points, cannot alter significantly the obtained results.

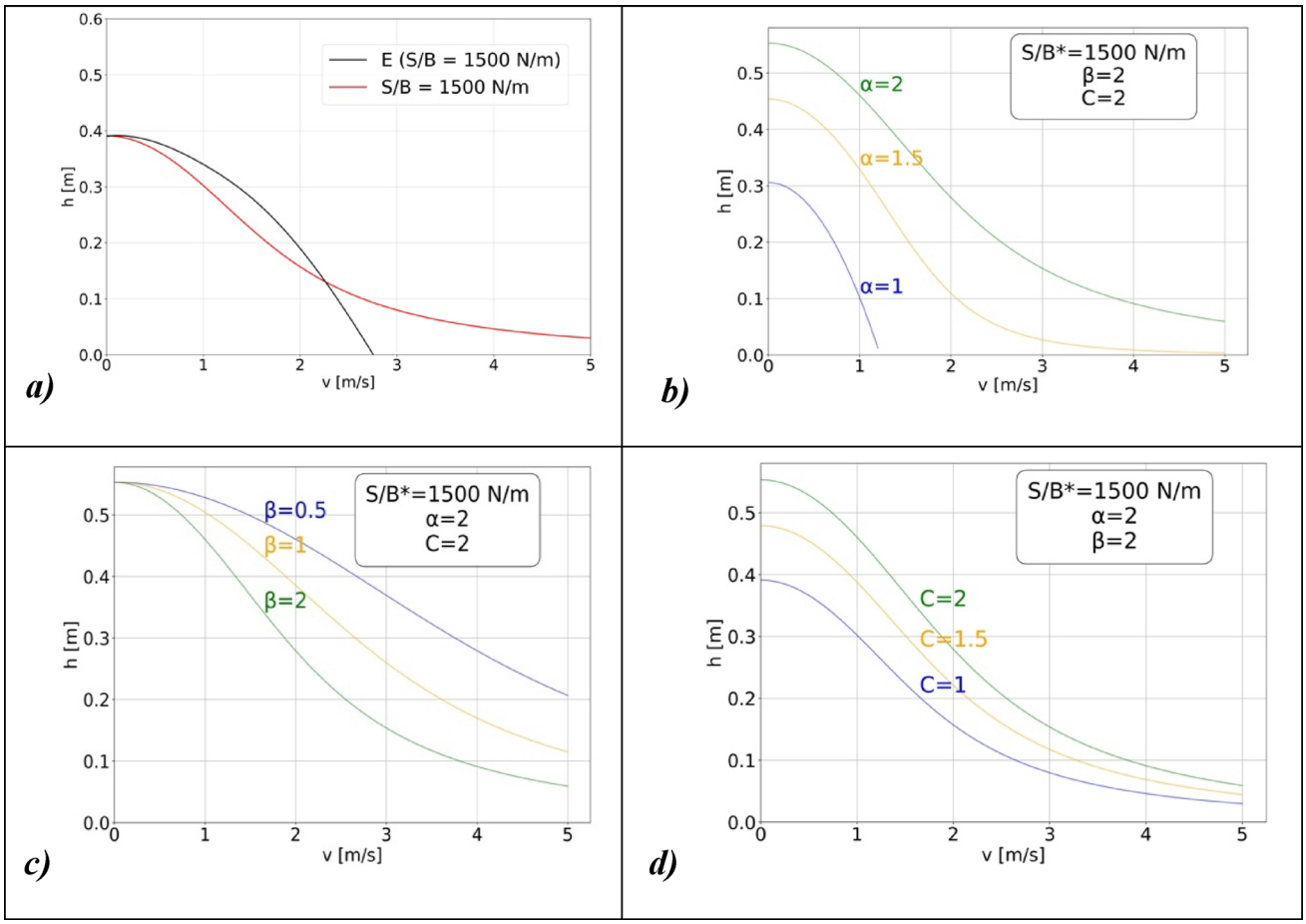

Fig. 2 S/B = 1500 N/m and relative E in a graph h-v (**a**); S/B* = 1500 N/m at different value of α (**b**), at different value of β (**c**), at different value of C (**d**)

During both the calibration and validation phases, we conducted a frequency analysis of the positions of *h-v* points relative to each generated S/B* curve. These curves were obtained using various *S/B** values (ranging from 500 to 3000 N/m) and different parameter coefficients. In this analysis involving the following steps, we identified: (i) the number of stable experimental points located below the curve, True Positives, *TP*, which represents the area deemed safe for pedestrians; (ii) the unstable experimental points below the curve, False Positives, *FP*, falling within the area identified as stable for pedestrians; and (iii) the number of unstable experimental points located above the curve—identified as True Negatives, *TN*— (iv) alongside the stable experimental points above the *S/B** curve, categorized as False Negatives, *FN*. This methodology allowed us to quantitatively assess the overall error associated with each curve, specifically the False Positives (overestimations of safety) and False Negatives (underestimations of stability) (Albano and Adamowsky 2025). As a result, we, firstly, selected the instability curves with a *Recall* (i.e. $TP/TP+FN$) value greater than 0.9 to minimize the error in predicting instable points during the calibration phase – it guarantees a condition of safety advantage. Among these selected curves, we then identified the one with the highest precision *Precision* (i.e. $TP/TP+FP$) aiming to reduce overestimation errors—i.e., inaccuracies in predicting pedestrian stability based on *h-v* points.

The *S/B** value that maximized these metrics was found to be *1400 N/m* with $\alpha = 2$ and $\beta = 2$ with C equal to 1.5. The chosen curve achieved an *Accuracy* (i.e. $TP+TN/TP+FP+FN+TN$) of 0.78 and 0.79, a *Precision* of 0.83 and 0.85, a *Recall* of 0.91 and 0.88 respectively in calibration and validation and an *F1* (*2 *(Precision*Recall)/(Precision+Recall)*) of 0,87 both phases.

The performance metrics of this S/B* curve were compared with those of physically-based approaches from the literature, specifically Lazzarin et al. (2022) and Milanesi et al. (2016), in terms of their ability to fit all the collected 417 experimental data. Figure 3 shows a radar graph with results of each metric for the three compared approaches; the *Precision* result is similar between the methods but the proposed

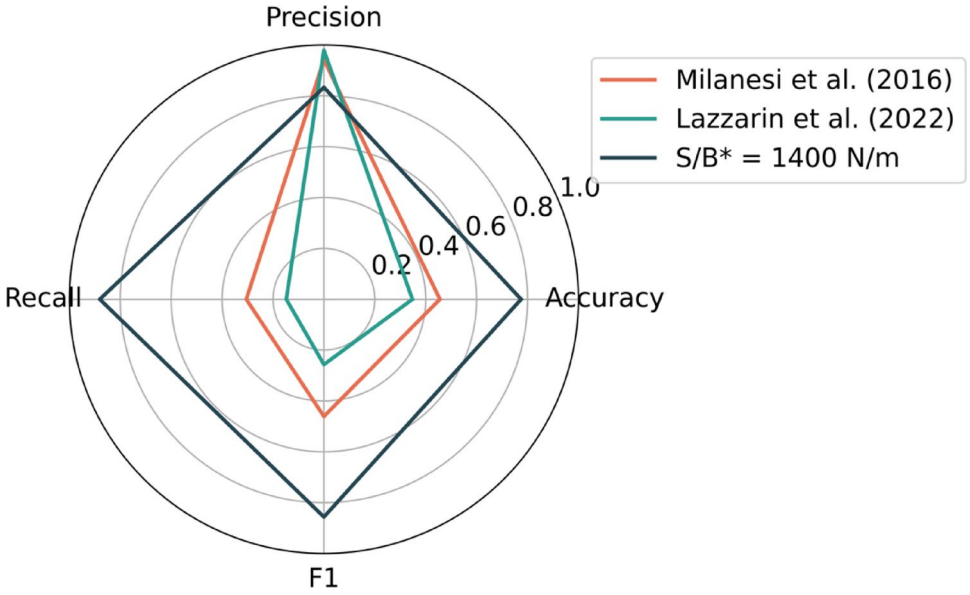

Fig. 3 Radar graph of the metrics results for the three compared physically-based instability curves

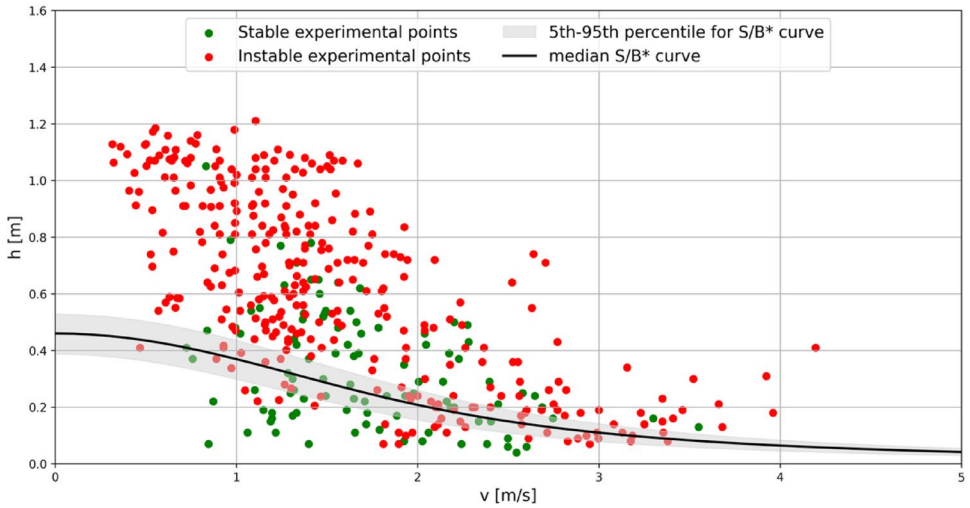

Fig. 4 Range of uncertainty of the instability curve S/B* = 1400 N/m with α=2 and β=2 varying parameter C on all the collected 417 experimental points

approach outperforms the others in terms of *Recall*, *Accuracy* and *F1*.

In a second phase, a confidence range of the selected *S/B** curve has been evaluated by varying the parameter *C* between 1 and 2 m with increments of 0.1 m. This involved evaluating the area between the 5th and 95th percentiles of the values obtained (Fig. 4).

The assessment of the confidence area overcomes the limit of the deterministic approach based on a single threshold, represented by a single instability curve. Indeed, the use of this confidence interval can reduce the influence of minor deviations in the values of *h* or *v* near the threshold defined by the curve, ensuring that the determination of actual pedestrian instability or stability conditions is not excessively affected by small fluctuations in these parameters.

Finally, an operational evaluation methodology based on the hydrodynamic parameters *h* and *v* was proposed for estimating the conditions under which pedestrians can safely stand versus those with a high probability of being swept away by flood events in urban areas. The *h*-*v* graph was divided into three hazard zones:

(i) The area of the graph above the 95th percentile in flow velocity is designated as the Unsafety Zone (shown in red in Fig. 5). In this zone, pedestrians face a high probability of instability.
(ii) The area between the 5th-95th percentile is categorized as the Uncertainty Zone (depicted in orange in Fig. 5). In this zone, pedestrians may experience potential instability.
(iii) The area below the 5th percentile curve is classified as the Safety Zone (represented in green in Fig. 5). In this zone, pedestrians have a low probability of instability.

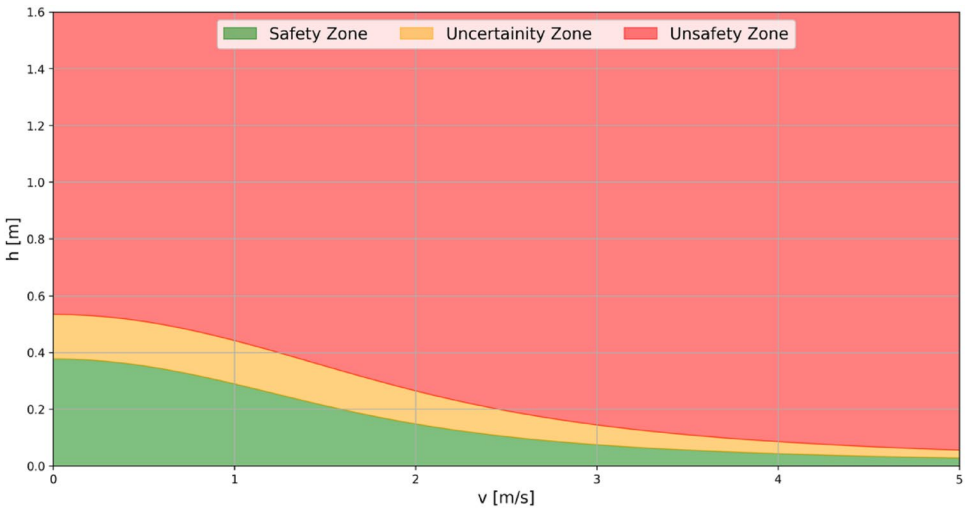

Fig. 5 Assessment of pedestrian instability hazard levels: safety zone (green), uncertainty zone (orange) and unsafe zone (red)

This classification facilitates a clearer understanding of pedestrian safety in flood-prone urban environments.

Benchmarking of *S/B** hazard thresholds on case study of Matera

The proposed method for identifying hazard threshold conditions—distinguishing safe pedestrian areas, the uncertainty zone and regions with a high probability of pedestrians being swept away by floods—was applied to the urban area of Matera, located in the Basilicata Region of southern Italy.

From an urban perspective, the most iconic part of Matera is the so-called "Sassi," the historic city canter characterized by rock-built structures. The "Sassi" was designated a UNESCO World Heritage Site in 1993, and Matera was named the European Capital of Culture for 2019. The "Sassi" is divided into two main historical districts: "Sasso Caveoso" and "Sasso Barisano". This case study focuses on the "Sasso Caveoso" urban basin, which covers approximately 0.66 km² and extends about 1.5 km longitudinally, with an average slope of 21.7% (Ermini and Albano 2023). In recent years, this area has experienced severe pluvial flooding, notably in 2018, 2019, 2023, and 2024, resulting in significant surface runoff and damage—including instances of people being trapped in their cars on flooded roads, losing their balance, and scooters being swept away.

Specifically, we used the November 2019 flood event maps of the envelope of the maximum water depth and the maximum flow velocity generated through a 2D hydraulic model simulation. These maps were employed to produce a hazard degree map based on the stability and instability conditions illustrated in Fig. 5.

The results demonstrated the effectiveness of the approach in identifying the most affected areas during the 2019 extreme rainfall event, as shown in Fig. 6. A key advantage of this method is the ability to pinpoint critical areas that may become inaccessible or roads that need to urgently restored. This information can assist decision-makers in prioritizing risk reduction measures during flood emergencies, especially when resources are limited. Overall, the approach shows great potential for supporting operational systems for near-real-time flood forecasting and monitoring.

Discussion

The methodology is transferable in other urban contexts, provided that the underlying assumptions of its development are consistently maintained. To this end, flood hazard criteria must satisfy several fundamental requirements to be effective and transferrable to other urban environments with different topographic or hydraulic characteristics. Firstly, they should be physically based, representing straightforward processes that stakeholders can easily understand. Secondly, the criteria should be user-friendly and offer understandable, simple to apply and graded vulnerability thresholds, allowing for adaptation to various environments, such as floodplains and mountainous regions, where flood behaviour can differ significantly. Lastly, these criteria should align reasonably well with experimental data while requiring minimal calibration to ensure reliability and practicality in diverse scenarios.

In this context, the proposed S/B* approach accounts for the mechanical action of a current, involving the combination of the thrust per unit width and the specific energy as critical hydraulic parameters that influence the in-stability of a person overwhelmed by floodwater. Moreover, we have used the coefficients α and β to refine the shape of the S/B* curve, enhancing its alignment with the experimental dataset through simple calibration. These coefficients can either increase or decrease the sensitivity of the hydrodynamic and

Fig. 6 Assessment of pedestrian stability and instability hazard levels in the "Sasso Caveoso" urban basin during the 2019 flood event

hydrostatic forces acting on the submerged object; consequently, the force becomes more sensitive to hydrodynamic action or velocity. Specifically, higher values of β cause the S/B* curve to be positioned along a path that indicates a generally lower water depth, while lower β values adjust the vertical pressure exerted on the object, taking into account the influence of the water column in relation to the object's weight. In particular, β varies between 0.5, which corresponds to the coefficient of Froud Number in the specific energy (E) formula, and 2, which aligns with unit thrust (S/B). Meanwhile, setting α to 1 causes the S/B* curve to converge with E, whereas setting α to 2 directs the curve toward S/B.

The use of a confidence range for the selected S/B* curve to delineate the uncertainty zone (in orange, as shown in Fig. 5) has been established by varying the parameter C between 1 and 2 m, which practically could be related to the height of individuals. This approach not only minimizes the deviation in the values of h or v near the defined curve threshold, ensuring that the actual determination of pedestrian instability or stability conditions is not excessively influenced by small fluctuations in these parameters, but it also offers a clear visual representation of risk levels in only 3 categories. By employing only three levels of hazard (green, orange, and red), this model simplifies the assessment, management, and communication of alerts, eliminating the need for multiple curves tailored to different demographic groups (e.g., women, men, children, the elderly, etc.) as such information is difficult to obtain for the aim of flood early warning system. This streamlined classification enhances clarity and facilitates effective decision-making immediately before or during a flood. To further complement this information, it is crucial to consider the number of individuals potentially present in the flooded area during a flood event. Therefore, mapping the spatial distribution of the flood instability and combining it with the presence of population is vital for effectively communicating flood risk to a wide audience. In this way, it is possible not only conveys the potential impact of flooding but also aids in crafting targeted response strategies to ensure public safety.

Another advantage of the proposed model is that the stability curves are directly influenced by the specific weight of the fluid, which impacts both the buoyancy and the dynamics of flow. Indeed, the increased sediment concentration in hyperconcentrated flow significantly enhances the drag force experienced by a person standing in such conditions. This effect is well known and underscores the importance of considering sediment concentration when evaluating stability in fluid environments. However, the work does not explicitly account for the local slope, representing a limitation. Usually, the reduction of stability due to the slope of the terrain is indirectly considered through velocity, which is a function of local slope. However, the explicit consideration of local slope in the formula, as well as the surface roughness, could increase the generalization to different

morphological situations, in particular in the range of low depths and high velocities, when the local slope is not negligible. This will be part of future research together with future applications to other kind of urban environment to demonstrate its relevance and adaptability.

Conclusions

The reliance on communication characterized by overly simplistic or alarmist messages can foster non-protective behaviors often resulting in excessive dependence on emergency management organizations or leads to dismissal of warnings and feelings of powerlessness. Conversely, providing overly detailed information, such as intricate data on hydraulic parameters like water depth and flow velocities, can be challenging for the general public—particularly non-experts—to comprehend (Albano et al. 2015).

Thus, it is essential to rethink our approach to communicating information to enhance awareness and effect meaningful changes in both individual and collective behaviors. Citizens must be empowered to assess the significance of potential flood events and understand when and how to implement life-saving measures.

To address this need, we propose a new methodology for assessing pedestrian instability based on the concept of tolerable thrust associated with a specific energy value, *S/B**. The *S/B** instability curve introduced in this study offers the advantage of being modeled based on three different parameters that consider the interplay of energy, flow velocity, and pedestrian characteristics. The optimal set of these parameters was defined based on experimental conditions and data collected from existing literature, through which the proposed methodology was validated to arrive at the definition of an optimal *S/B** curve.

This approach aims to establish a technical-practical framework that supports emergency management by enhancing accessibility and enabling effective recovery. It can help to identify urban areas most susceptible to flooding during events as it has been showed for the case study of Matera urban area. In particular, hazard thresholds were evaluated through a combination of water depth and flow velocity. In the future, we plan to incorporate friction and slope terms into the S/B* equation to make it more applicable to various urban contexts and enhance its predictive accuracy. Nonetheless, the current equation remains cost-effective and easily generalizable, requiring only a few parameters and constraints.

The methodology can be applied to urban contexts other than the one investigated in this study, provided that the underlying assumptions of its development are respected.

The impact of this study is to enhance preparedness and safety for pedestrians in flood-prone urban areas, providing valuable support to emergency management decision-makers in tasks such as placing warning signals and designing evacuation routes.

Acknowledgements This work was funded by the Next Generation EU - Italian NRRP, Mission 4, Component 2, Investment 1.5, call for the creation and strengthening of 'Innovation Ecosystems', building 'Territorial R&D Leaders' (Directorial Decree n. 2021/3277) - project Tech4You - Technologies for climate change adaptation and quality of life improvement, n. ECS0000009. This work reflects only the authors' views and opinions, neither the Ministry for University and Research nor the European Commission can be considered responsible for them.

Author contributions Conceptualization (R.A.); Data curation (R.A); methodology (R.A., T.M.); formal analysis (R.A.; E.R.); writing - original draft and editing (R.A, E.R., T.M.); writing—review and editing (R.A, E.R., T.M., A.S.); funding acquisition, (R.A.). All authors have read and agreed to the published version of the manuscript.

Funding Open access funding provided by Università degli Studi della Basilicata within the CRUI-CARE Agreement.

Data availability The original contributions presented in the study are included in the article; further inquiries can be directed to the corresponding author.

Declarations

Conflict of interest The authors declare no competing interests.

References

Abt SR, Wittier RJ, Taylor A, Love DJ (1989) Human stability in a high flood hazard zone. J Am Water Resour Assoc 25:881–890. https://doi.org/10.1111/j.1752-1688.1989.tb05404.x

Albano R, Adamowski J (2025) Use of digital elevation models for flood susceptibility assessment via a hydrogeomorphic approach: a case study of the Basento River in Italy. Nat Hazards. https://doi.org/10.1007/s11069-025-07144-z

Albano R, Sole A, Adamowski J, Mancusi L (2014) A GIS-based model to estimate flood consequences and the degree of accessibility and operability of strategic emergency response structures in urban areas. Nat Hazards Earth Syst Sci 14:2847–2865. https://doi.org/10.5194/nhess-14-2847-2014

Albano R, Sole A, Adamowski J (2015) READY: a web-based geographical information system for enhanced flood resilience through raising awareness in citizens. Nat Hazards Earth Syst Sci 15:1645–1658. https://doi.org/10.5194/nhess-15-1645-2015

Arrighi C, Oumeraci H, Castelli F (2017) Hydrodynamics of pedestrians' instability in floodwaters. Hydrol Earth Syst Sci 21:515–531. https://doi.org/10.5194/hess-21-515-2017

Chanson H, Brown R (2014) Turbulence in an inundated urban environment during a major flood: implications in terms of people evacuation and sediment deposition. Mech Ind 15:101–106. https://doi.org/10.1051/meca/2014017

Ermini R, Albano R (2023) Hydromorphic analysis of urban areas transformations: the case study of the Matera city. In: IOP conference series: earth and environmental science, vol 1196

European Commission: Joint Research Centre, Ehrlich D, Kemper T, Uhl J, Marí Rivero I et al. (2024) Atlas of the human planet 2024. In: Ehrlich D, Kemper T(eds) Publications Office of the European Union. https://data.europa.eu/doi/10.2760/808886

Foster DN, Cox RJ (1973) Stability of children on roads used as floodways. Technical report no. 73/13, Water Research Laboratory of the University of New South Wales, Manly Vale, Australia

Ipcc (2022) Global warming of 1.5°C: IPCC special report on impacts of global warming of 1.5°C above pre-industrial levels in context of strengthening response to climate change, sustainable development, and efforts to eradicate poverty, 1st edn. Cambridge University Press. https://doi.org/10.1017/9781009157940

Jonkman SN, Penning-Rowsell E (2008) Human instability in flood flows[1]. J Am Water Resour Assoc 44:1208–1218. https://doi.org/10.1111/j.1752-1688.2008.00217.x

Karvonen RA, Hepojoki HK, Huhta HK, Louhio A (2000) The use of physical models in dam-break flood analysis, development of rescue actions based on dam-break flood analysis (RESCDAM). Final report, Helsinki University of Technology, Finnish Environment Institute, Helsinki, Keller and Mitsch, Melbourne, Australia

Lazzarin T, Viero DP, Molinari D, Ballio F, Defina A (2022) Flood damage functions based on a single physics- and data-based impact parameter that jointly accounts for water depth and velocity. J Hydrol 607:127485. https://doi.org/10.1016/j.jhydrol.2022.127485

Lechowska E (2018) What determines flood risk perception? A review of factors of flood risk perception and relations between its basic elements. Nat Hazards 94:1341–1366. https://doi.org/10.1007/s11069-018-3480-z

Martínez-Gomariz E, Gómez M, Russo B (2016) Experimental study of the stability of pedestrians exposed to urban pluvial flooding. Nat Hazards 82:1259–1278. https://doi.org/10.1007/s11069-016-2242-z

Milanesi L, Pilotti M, Ranzi R (2015) A conceptual model of people's vulnerability to floods. Water Resour Res 51:182–197. https://doi.org/10.1002/2014WR016172

Milanesi L, Pilotti M, Bacchi B (2016) Using web-based observations to identify thresholds of a person's stability in a flow: web observations of a person's stability in a flow. Water Resour Res 52:7793–7805. https://doi.org/10.1002/2016WR019182

Moramarco T (2011) Fasce di pericolosità idraulica e criteri per l'individuazione di aree marginali

RESCDAM - Development of Rescue Actions Based on Dam-Break Flood Analysi\ s (n.d)

Russo B, Gómez M, Macchione F (2013) Pedestrian hazard criteria for flooded urban areas. Nat Hazards 69:251–265. https://doi.org/10.1007/s11069-013-0702-2

Sole A, Giosa L, Albano R, Cantisani A (2013) The laser scan data as a key element in the hydraulic flood modelling in urban areas. Int Arch Photogramm Remote Sens Spat Inf Sci XL-4/W1:65–70. https://doi.org/10.5194/isprsarchives-XL-4-W1-65-2013

Takahashi S, Endoh K, Muro ZI (1992) Experimental study on people's safety against overtopping waves on breakwaters. Report on the Port and Harbour Institute, Report 031-04-01 Yokosuka, Japan

UNISDR (2015) Sendai framework for disaster risk reduction 2015–2030. United Nations Office for Disaster Risk Reduction (UNISDR), p 32. https://www.unisdr.org/we/inform/publications/43291

Winsemius H, Aerts J, van Beek L et al (2016) Global drivers of future river flood risk. Nat Clim Change 6:381–385. https://doi.org/10.1038/nclimate2893

Xia J, Falconer RA, Wang Y, Xiao X (2014) New criterion for the stability of a human body in floodwaters. J Hydraul Res 52:93–104. https://doi.org/10.1080/00221686.2013.875073

Yee M (2003) Human stability in floodways. Undergraduate honors Thesis, School of civil and environmental engineering, University of New South Wales, Australia

Zhu Z, Zhang Y, Gou L, Peng D, Pang B (2023) On the physical vulnerability of pedestrians in urban flooding: experimental study of the hydrodynamic instability of a human body model in floodwater. Urban Clim 48:101420. https://doi.org/10.1016/j.uclim.2023.101420